Experimental investigation of different regimes of mode-locking in a high repetition rate passively mode-locked semiconductor quantum-dot laser

Fabien Kéfélian, Shane O'Donoghue, Maria Teresa Todaro, John G. Mcinerney, Guillaume Huyet

Experimental investigation of different regimes of mode-locking in a high repetition rate passively mode-locked semiconductor quantum-dot laser

Fabien Kéfélian[1,3], Shane O'Donoghue[1,2], Maria Teresa Todaro[2,4], John McInerney[2] and Guillaume Huyet[1]

[1]*Tyndall National Institute and Cork Institute of Technology*
Lee Maltings Photonics Building, Prospect Row, Cork, Ireland

[2]*Tyndall National Institute and Department of Physics, University College Cork*
Lee Maltings Photonics Building, Prospect Row, Cork, Ireland

[3]*Currently with Université Paris-XIII*
99, rue Jean-Baptiste Clément, 93430 Villetaneuse, France

[4]*Currently with National Nanotechnology Laboratory, National Institute for the Physics of Matter and Universita di Lecce*
Via Arnesano, 73100 Lecce, Italy
huyet@tyndall.ie

Abstract: We report experimental investigations on a two-section 16-GHz repetition rate InAs/GaAs quantum dot passively mode-locked laser. Near the threshold current, pseudo-periodic Q-switching with complex dynamics is exhibited. Mode-locking operation regimes characterized by different repetition rates and timing jitter levels are encountered up to twice the threshold current. Evolution of the RF spectrum and optical spectrum with current is compared. The different mode-locked regimes are shown to be associated with different spectral and temporal shapes, ranging from 1.3 to 6 ps. This point is discussed by introducing the existence of two different supermodes. Repetition rate evolution and timing jitter increase is attributed to the coupling between the dominant and the secondary supermodes.

OCIS codes: (140.5960) semiconductor lasers; (140.4050) mode-locked lasers

References and links

1. N. Yamada, H. Ohta, and S. Nogiwa, "Jitter-free optical sampling system using passively modelocked fibre laser," Electron. Lett. **38**, 1044–1045 (2002).
2. P. Delfyett, D. Hartman, and S. Ahmad, "Optical clock distribution using a mode-locked semiconductor laser-diode system," J. Lightwave Technol. **9**, 1646–1649 (1991).
3. L. A. Jiang, E. P. Ippen, and H. Yokoyama, "Semiconductor mode-locked lasers as pulse sources for high bit rate data transmission," Journal of optical and fiber communications reports **2**, 1–31 (2005).
4. P. E. Barnsley, H. J. Wickes, G. E. Wickens, and D. M. Spirit, "All-optical clock recovery from 5 Gb/s RZ data using a self-pulsating 1.56 μm laser diode," IEEE Photon. Technol. Lett. **3**, 942–945 (1991).
5. A. Schliesser, M. Brehm, F. Keilmann, and D. van der Weide, "Frequency-comb infrared spectrometer for rapid, remote chemical sensing," Opt. Express **13**, 9029–9038 (2005).

#102295 - $15.00 USD Received 2 Oct 2008; revised 4 Dec 2008; accepted 7 Dec 2008; published 2 Apr 2009

6. A. Major, V. Barzda, P. A. E. Piunno, S. Musikhin, and U. J. Krull, "An extended cavity diode-pumped femtosecond Yb:KGW laser for applications in optical DNA sensor technology based on fluorescence lifetime measurements," Opt. Express **14**, 5285–5294 (2006).
7. K. A. Williams, M. G. Thompson, and I. H. White, "Long-wavelength monolithic mode-locked diode lasers," New J. Phys. **6**, 179 (2004).
8. E. P. Ippen, "Principles of passive mode locking," Appl. Phys. B **58**, 159–170 (1994).
9. P. T. Ho, L. A. Glasser, E. P. Ippen, and H. A. Haus, "Picosecond pulse generation with a cw (GaAl)As laser diode," Appl. Phys. Lett. **33**, 241–243 (1978).
10. X. Huang, A. Stintz, H. Li, L. F. Lester, J. Cheng, and K. J. Malloy, "Passive mode-locking in 1.3 μm two-section InAs quantum dot lasers," Appl. Phys. Lett. **78**, 2825–2827 (2001).
11. D. Bimberg, M. Kuntz, and M. Laemmlin, "Quantum dot photonic devices for lightwave communication," Appl. Phys. A **80**, 1179–1182 (2005).
12. H. A. Haus, "Theory of mode locking with a fast saturable absorber," J. Appl. Phys. **46**, 3049–3058 (1975).
13. H. A. Haus, "A theory of forced mode locking," IEEE J. Quantum Electron. **11**, 323–330 (1975).
14. H. A. Haus, "Parameter ranges for CW passive mode locking," IEEE J. Quantum Electron. **12**, 169–176 (1976).
15. J. Mulet and J. Moerk, "Analysis of timing jitter in external-cavity mode-locked semiconductor lasers," IEEE J. Quantum Electron. **42**, 249–256 (2006).
16. M. T. Todaro, J.-P. Tourrenc, S. P. Hegarty, C. Kelleher, B. Corbett, G. Huyet, and J. G. McInerney, "Simultaneous achievement of narrow pulse width and low pulse-to-pulse timing jitter in 1.3μm passively mode-locked quantum-dot lasers," Opt. Lett. **31**, 3107–3109 (2006).
17. E. Viktorov, P. Mandel, M. Kuntz, G. Fiol, D. Bimberg, A. G. Vladimirov, and M. Wolfrum, "Stability of the modelocking regime in quantum dot laser," in *CLEO/Europe-IQEC* (2007).
18. M. J. R. Heck, E. A. Bente, B. Smalbrugge, Y.-S. Oei, M. K. Smit, S. Anantathanasarn, and R. Notzel, "Observation of Q-switching and mode-locking in two-section InAs/InP (100) quantum dot lasers around 1.55 μm," Opt. Express **15**, 16,292–16,301 (2007).
19. F. Kéfélian, S. O'Donoghue, M. T. Todaro, J. McInerney, and G. Huyet, "RF Linewidth in Monolithic Passively Mode-Locked Semiconductor Laser," IEEE Photon. Technol. Lett. **20**, 1405–1407 (2008).
20. O. McDuff and S. E. Harris, "Nonlinear theory of the internally loss-modulated laser," IEEE J. Quantum Electron. **3**, 101–111 (1967).
21. H. Haken and M. Pauthier, "Nonlinear theory of multimode action in loss modulated lasers," IEEE J. Quantum Electron. **4**, 454–459 (1968).
22. J. R. Fontana, "Theory of spontaneous mode locking in lasers using a circuit model," IEEE J. Quantum Electron. **8**, 699–703 (1972).
23. J. A. Yeung, "Theory of active mode-locking of a semiconductor laser in an external cavity," IEEE J. Quantum Electron. **17**, 398–404 (1981).
24. K. Y. Lau, "Narrow-Band Modulation of semiconductor lasers at millimeter wave frequencies (>100 GHz) by mode locking," IEEE J. Quantum Electron. **26**, 250–261 (1990).
25. A. E. Siegman and D. J. Kuizenga, "FM and AM mode-locking of the Homogeneous Laser. I. Theory," IEEE J. Quantum Electron. **6**, 2088–2091 (1970).
26. H. A. Haus, "Theory of mode locking with a slow saturable absorber," IEEE J. Quantum Electron. **11**, 736–746 (1975).
27. E. A. Avrutin, J. H. Marsh, and E. L. Portnoi, "Monolithic and multi-GHz mode locked semiconductor lasers: experiment, modeling and applications," Proc. IEE Optoelectronics **147**, 251–278 (2000).
28. H. A. Haus and A. Mecozzi, "Noise of mode-locked lasers," IEEE J. Quantum Electron. **29**, 983–996 (1993).
29. I. Kim and K. Y. Lau, "Frequency and timing stability of mode-locked semiconductor lasers–Passive and active mode locking up to millimeter wave ferquencies," IEEE J. Quantum Electron. **29**, 1081–1090 (1993).
30. R. Adler, "A study of locking phenomena in oscillators," in *Proceedings IRE*, vol. 34, pp. 351–356 (1946).
31. K. Y. Lau and J. Paslaski, "Condition for short pulse generation in ultrahigh frequency mode-locking of semiconductor lasers," IEEE Photon. Technol. Lett. **3**, 974–976 (1991).

1. Introduction

High repetition rate optical pulse sources are critical for advancement in diverse applications such as optical sampling [1], clocking [2], optical time-division multiplexing [3], clock recovery and frequency conversion [4], radar and remote sensing [5], and medical diagnostics [6]. In all these applications, combining few ps pulsewidth and sub-ps timing jitter is essential. Monolithic mode-locked semiconductor lasers are becoming increasingly attractive to provide stable and reliable pulse trains with multi-GHz repetition rates [7]. Passive mode-locking can be achieved simply in these lasers by designing two electrically isolated sections and applying a reverse voltage to one of them to obtain an intracavity saturable absorber. Passively mode-

#102295 - $15.00 USD Received 2 Oct 2008; revised 4 Dec 2008; accepted 7 Dec 2008; published 2 Apr 2009

locked lasers, where pulses modulate the absorption on their own, yield much shorter pulses and higher repetition rates than actively mode-locked lasers, without any external electrical oscillator [8], although sometimes at the expense of higher timing jitter.

Monolithic mode-locked picosecond pulse diode lasers have been realized since 1978 [9] with bulk devices, then with quantum wells [7] and more recently with quantum dots [10]. Quantum-dot lasers demonstrate numerous advantages over bulk and quantum well lasers such as low wavelength chirp, low threshold currents and reduced linewidth enhancement factor [11]. In addition to these advantages, their broad gain spectra (due to dot size dispersion and shape) and easy absorption saturation make them well suited to mode-locking and broadband applications.

Stable operation in passively mode-locked laser is generally limited to small ranges of gain and saturable loss parameters [12] [13] [14]. Indeed, CW steady-state single pulse mode-locked solutions have to satisfy various different criteria of existence and stability and can easily be degraded or prevented by perturbations, such as relaxation oscillations, or may not be self-starting. Q-switching or self-pulsation can thus occur, especially at high power.

Understanding, improving and controlling the timing jitter is essential to improve performance, manufacturability and widespread use of mode-locked lasers in real applications. One of the most challenging problems is to achieve simultaneously very narrow pulses, low timing jitter and sufficient optical power (0.1-1 W for realistic applications). Recently, both simulations [15] and experiments [16] have exhibited ”incomplete”, partially stable, mode-locking regimes at high powers. The origin and characteristics of this regime in quantum-dot lasers have yet to be investigated. In this paper we report an extended study of the different operation regimes encountered in a two-section quantum dot passively mode-locked laser, based on experimental measurements of the optical spectrum, radio-frequency (RF) spectrum, timing pulsewidth and pulseshape, for different gain and absorption settings.

2. Experimental measurements and discussions

2.1. Threshold and switching regime

The device analyzed is a two-section InAs/GaAs quantum-dot laser emitting near 1.3 μm similar to that of [16]. The molecular-beam-epitaxy-grown wafer was supplied by NL Nanosemiconductor GmbH. The active region consists of 10 layers of InAs quantum dots separated by 33 nm of GaAs and bounded by $Al_{0.35}Ga_{0.65}As$ cladding layers. The absorber section represents 30% of the 2.5-mm total length of the cavity resulting in a repetition rate of 16.2 GHz.

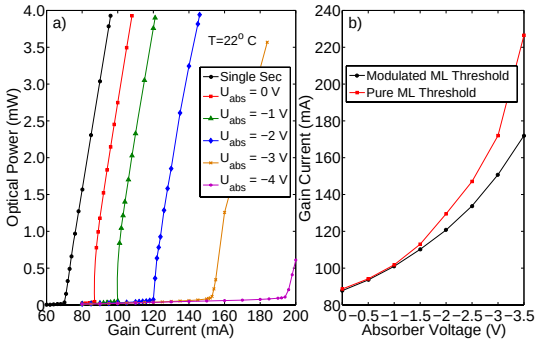

Fig. 1. Average optical power versus gain current for different absorber voltage (a) and threshold currents as a function of the absorber voltage (b)

#102295 - $15.00 USD Received 2 Oct 2008; revised 4 Dec 2008; accepted 7 Dec 2008; published 2 Apr 2009

Fig. 1(a) presents laser average optical power versus gain current for different values of the absorber section voltage. Unlike in conventional single section lasers, the light power vs current curve exhibits a sharp increase at the threshold. Using a second-harmonic-generation autocorrelator, pico-second pulses are detected which demonstrates mode-locked operation. This is confirmed by the existence of a peak in the RF spectrum at the cavity roundtrip frequency. The analysis of the average output optical power using a photo-diode coupled to a 500-MHz bandwidth oscilloscope shows the appearance of pseudo-periodic switches between the mode-locked regime and the non-lasing state. Mode-locking modulated by Q-switching has been observed in InAs/InGaAs quantum-dot two-section laser [17] and theoretical works [12] [13] [14] on mode-locked lasers have demonstrated a range of currents in which optical bistability between non-lasing and mode-locking occurs. The pseudo-periodic switches observed experimentally can therefore be explained by noise-coupled bistability between mode-locked and non-lasing states, associated with Q-switching modulation.

Fig. 1(b) shows the range of currents where modulated mode-locking is observed as a function of the absorber voltage. The lower curve corresponds to the modulation appearence (modulated mode-locking threshold) and the upper curve corresponds to the current for which modulation disappears (pure mode-locking threshold). The difference between the two threshold intensities increases with the reverse absorber voltage. Fig. 2 presents the different switching

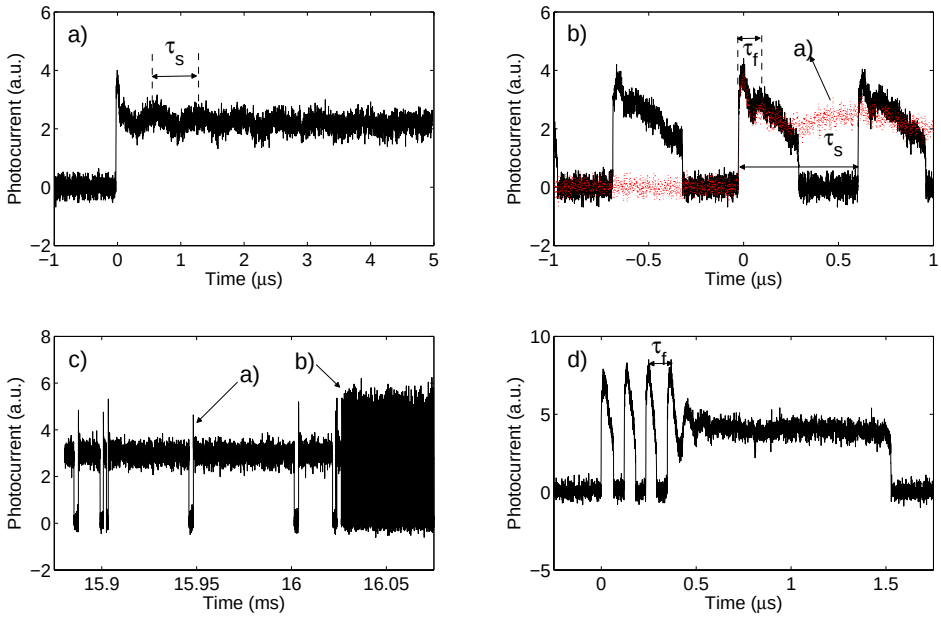

Fig. 2. Photocurrent temporal dynamics closed to the lasing treshold

regimes encountered when current is increased, showing both fast and slow switches. Fig. 2(a) shows a switch between lasing and non lasing states with damped oscillations of period τ_s from 750 to 630 ns, when the absorber voltage varies from 0 V to - 3 V, and a damping time of 6 μs. Fig. 2(b) presents switching during the first $\tau_s/2$ half cycle and features faster oscillations with a period τ_f=100 ns. The dotted line in Fig. 2(b) shows the lasing and non lasing state switching superimposed on the $\tau_s/2$ half cycle switch, and shows the similarity between the

#102295 - $15.00 USD Received 2 Oct 2008; revised 4 Dec 2008; accepted 7 Dec 2008; published 2 Apr 2009

switch times and the maxima and minima of the slow oscillation. At higher current and reverse bias settings the two switches can behave simultaneously and Fig. 2(c) presents a succession of switches of kind a) followed by switches of kind b) (not resolved with this time scale). Fig. 2(d) shows the fast oscillations switch of period τ_f followed by damped oscillations of kind a). These switching patterns are somewhat similar to the ones shown in Fig. 4(b) of [18] with three main differences, the time scale is here 10 times slower, the modulation is not purely periodic but pseudo-periodic and it corresponds to mode-locking modulated by Q-switching and not to pure Q-switching.

2.2. RF characterization of the mode-locking regime

The mode-locked operation is detected and characterized using a high speed detector and a 25-GHz bandwidth electrical spectrum analyzer. The power spectral density of the first harmonic of

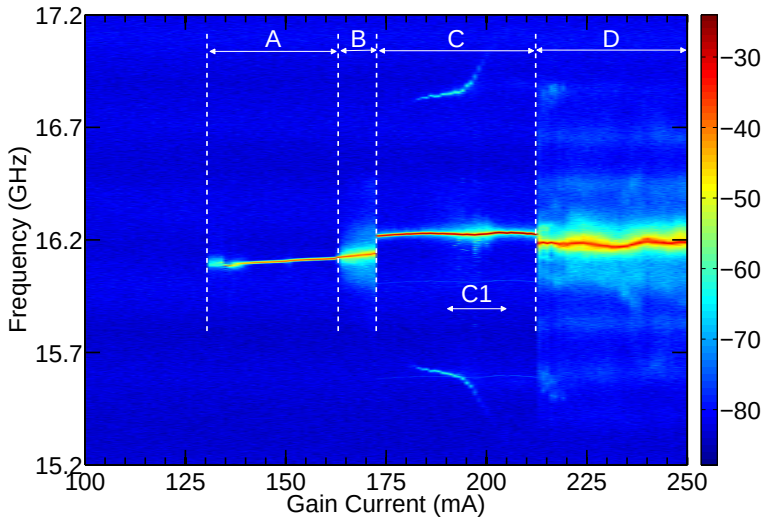

Fig. 3. RF spectrum in dB scale as a function of the gain current, U_{abs}=-2.4 V

the photocurrent (RF spectrum) is measured for a large range of currents and different absorber voltages. Fig. 3 shows the results of these measurements for an absorber voltage of -2.4 V. The presence of a clear peak in the RF spectrum around 16.2 GHz indicates mode-locking in a broad range of currents above mode-locking threshold. However, the RF spectrum exhibits different shapes which may correspond to different regimes or types of mode-locking. For a range of currents between the threshold current and 163 mA (range A), the RF spectrum is a very narrow line (from several kHz to several tens of kHz [19]) whose central frequency (i.e. pulse train repetition rate) increases with the current. At 163 mA, the RF central frequency versus current exhibits a slope discontinuity and the RF spectrum starts to broaden with current until 175 mA (range B). At this current, the central frequency of the RF spectrum jumps to a higher value and exhibits a narrow lineshape as in the first range of currents. In addition, the RF spectrum features side-bands at frequencies between 600 and 800 MHz from the central frequency (range C). Finally, at 195 mA, the RF central frequency jumps back to the initial central frequency and the RF spectrum becomes very broad (range D). The same measurements for an absorber voltage of -2.3 V are presented on Fig. 4. We encounter the same succession of regimes except that in the range C the photocurrent exhibits a noisier spectrum with small

#102295 - $15.00 USD Received 2 Oct 2008; revised 4 Dec 2008; accepted 7 Dec 2008; published 2 Apr 2009

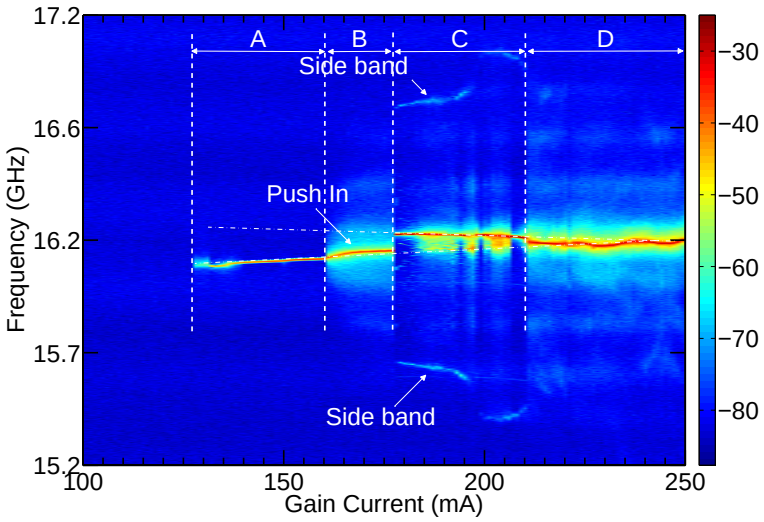

Fig. 4. RF spectrum in dB scale as a function of the gain current, U_{abs}=-2.3 V

ranges of switching between two central frequencies.

2.3. Discussion on the RF characterization results

Two approaches exist for the theoretical investigation of mode-locking, time domain and frequency domain (or coupled-mode equation). The frequency domain approach for active mode-locking was first introduced by McDuff and Harris [20] and developed analytically by Haken and Pauthier [21]. For passive mode-locking using a saturable absorber, a frequency domain theory using a circuit model was presented by Fontana [22]. Frequency domain theory was developed by Yeung [23] for active mode-locking of a semiconductor laser and by Lau [24] for active and passive mode-locking of a semiconductor laser at high repetition rate. The time domain approach theory was developed for active mode-locking by Siegman and Kuizenga [25] and for passive mode-locking by Haus for both fast [12] and slow [26] saturable absorbers. Additionally, both approaches for passive mode-locking have been compared by Haus [13]. Numerous numerical models have been developed in the two domains for active, passive, hybrid and harmonic mode-locking in diode laser (see [27] for an overview).

For the investigation of noise in mode-locked laser, a slow time variable is generally introduced in both approaches leading to a set of temporal coupled-mode equations in the frequency domain or a double variable temporal equation for the time domain approach using a short term time variable as well as a time variable on the scale of many cavity round trip-times. A theory of noise in passively mode-locked lasers (concerning pulse energy, phase, timing and frequency) has been developed by Haus and Mecozzi [28]. A completely different theory for frequency and temporal noises using frequency domain approach and excitation of unstable solutions of the coupled-mode equations has been simultaneously proposed by Kim and Lau for active and passive mode-locking in semiconductor laser at high repetition rate [29].

To analyze the results of these measurements, we will use the latter frequency domain approach and particularly the concept of ”supermode”. A supermode is here defined as a set of longitudinal modes equally spaced and locked in a fixed phase relationship. It is a solution of the coupled-mode equation for the intracavity electric field. Each supermode has an associated

#102295 - $15.00 USD Received 2 Oct 2008; revised 4 Dec 2008; accepted 7 Dec 2008; published 2 Apr 2009

repetition frequency, equal to the frequency interval between the modes, and a threshold. In the time domain, a supermode corresponds to a train of pulses of specific duration and repetition rate. The repetition frequency is generally detuned compared to the free spectral range of the cavity. In [29] the Hermite-Gaussian supermode expansion from [21] is used, which is the result of an assumed parabolic optical gain spectrum and a sinusoidal gain modulation at the cavity mode frequency spacing. This is a very idealized representation, indeed passively mode-locked diode lasers generally exhibit asymetric gain curve, dispersion, index-gain coupling factor. Moreover gain modulation and shaping, the latter resulting from self action of the pulse train on the gain and the absorber media, is sharper than a sinusoid. As a result, a realistic supermode expansion should involve supermodes with different mode separation frequencies.

We analyze consequently the results presented on Fig. 3 and Fig. 4 while considering the existence of two supermodes. The range A represents a single supermode regime, i.e. the existence of only one supermode called SM1. The repetition frequency of the supermode SM1 changes with the current due to the refractive index change and the pulse energy change. The range C also corresponds to a single supermode regime, with the supermode SM2. SM2 has a repetition frequency greater than SM1. On Fig. 4 we have extrapolated (dash lines) the linear slope of the repetition frequency of SM1 and SM2. Range B exhibits a nonlinear variation of the repetition frequency of SM1 which is similar to the push-in effect in an oscillator submitted to the injection of a master oscillator with a frequency difference close to the locking range [30]. Consequently we interpret the peculiar central frequency evolution in the range B as the effect of the non lasing supermode SM2 on the lasing supermode SM1, leading to a push-in of the repetition frequency and a sudden rise of the noise. The same interpretation can be given for the regime C1 on Fig. 3. The main difference between the results of -2.4 V and -2.3 V is the behavior in the central region C. For -2.3 V the laser does not exhibit a clear single SM2 supermode behavior, the perturbation induced by the supermode SM1 can be clearly seen. Moreover, the variation of the repetition frequency versus current for SM1 and SM2 appears to be of contrary signs on Fig. 4. The range D exhibits the supermode SM1, strongly perturbed by the non-lasing supermode SM2.

2.4. Optical spectrum characterization

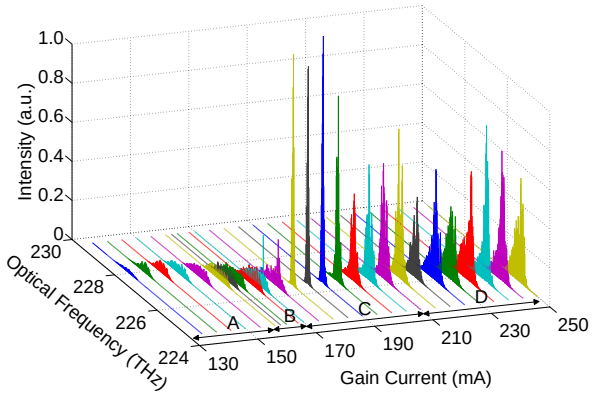

Fig. 5. Optical spectrum as a function of the gain current, U_{abs}=-2.4 V

To confirm our interpretation of the measurements in the RF domain, we have recorded the optical spectrum for the same range of currents. Fig. 5 presents the results for an absorber volt-

#102295 - $15.00 USD Received 2 Oct 2008; revised 4 Dec 2008; accepted 7 Dec 2008; published 2 Apr 2009

age of -2.4 V. Transition of regime between range B and C is obvious and confirms the existence of two different supermodes. Transition between range A and B is characterized by a shift of the central frequency of the optical spectrum envelope toward the central optical frequency of SM2. Moreover these measurements show that the shift of the central RF frequency presented in Fig. 3 cannot be explained simply by the optical frequency shift coupled to the dispersion.

2.5. Pulseshape characterization

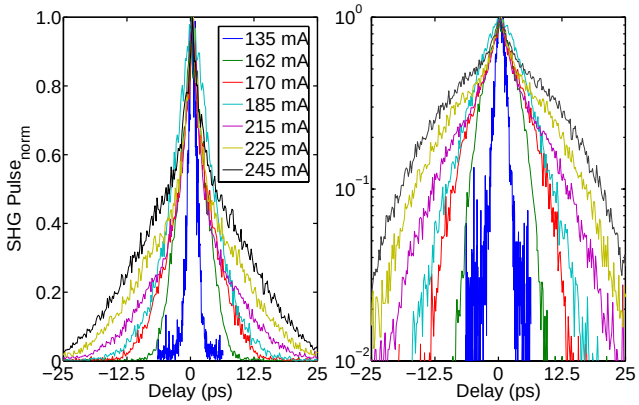

Fig. 6. Pulse autocorrelation for different gain currents in linear (left) and logarithmic (right) scales for U_{abs}=-2.4 V .

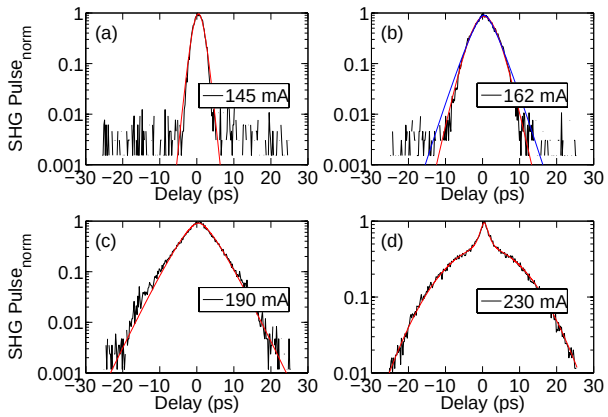

Fig. 7. Experimental pulse autocorrelation and fit for different gain currents and fitting curves for U_{abs}=-2.4 V. a) is a square hyperbolic secant autocorrelation fit, b) is a a square hyperbolic secant autocorrelation fit (red) and a symmetric two-sided inverse exponential autocorrelation fit (blue), c) is a symmetric two-sided inverse exponential autocorrelation fit and d) is a symmetric two-sided inverse exponential autocorrelation fit on a Gaussian pedestal

To understand the relation between the different regimes observed on the RF spectra, and the pulse properties, we have measured, with a non-collinear (background-free) second-harmonic generation autocorrelator, the autocorrelation of the pulse for the same range of currents. Each

#102295 - $15.00 USD Received 2 Oct 2008; revised 4 Dec 2008; accepted 7 Dec 2008; published 2 Apr 2009

regime has a different pulse shape associated to it and the results are summarized on Fig. 6 and Fig. 7. The first shape encountered in current range A (I=135 mA in Fig. 6) is correctly fitted by the autocorrelation of a square hyperbolic secant function (Fig. 7(a)). The second shape, encountered in current range B (I=162 mA and 170 mA plots in Fig. 6) is an intermediate between the autocorrelation of a square hyperbolic secant function and the autocorrelation of a symmetric two-sided inverse exponential function (Fig. 7(b)). The third shape, encountered in the first part of range C (I=185 mA in Fig. 6), is well fitted by the autocorrelation of a symmetric two-sided exponential function (Fig. 7(c)). Finally the last shape, encountered after I=190 mA (I=215, 225 and 245 mA in Fig. 6), presents a symmetric two-sided inverse exponential center and a Gaussian pedestal (Fig. 7(d)).

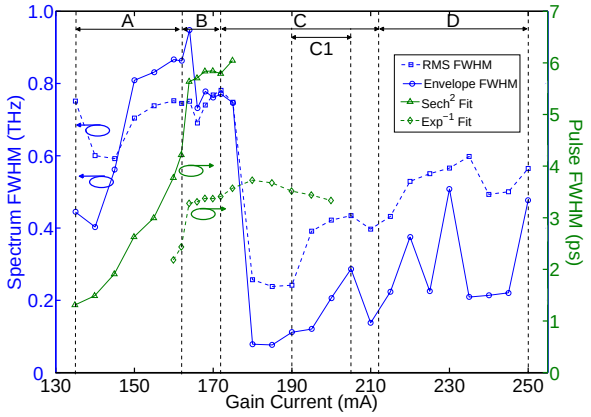

Fig. 8. Pulse and spectrum full width at half maximum as a function of the gain current

Fig. 8 presents simultaneously the width of the optical pulse and the width of the optical spectrum. The spectrum width is given by two quantities, the RMS width and the envelope full width at half maximum (FWHM). For the regimes where the autocorrelation can be fitted with a single function (region A and C) the FWHM of the pulse was derived from the autocorrelation FWHM. For the shape encountered in current range B, we have plotted the FWHM calculated with a square hyperbolic secant fit and a symmetric two-sided inverse exponential fit, so this data is consequently to be taken with caution. In the current range A, the pulse FWHM increases quadratically with current while the spectrum also broadens. This indicates a strong rise of the pulse chirp with current ($\Delta\nu\Delta\tau$=3.2 at I=160 mA). In the current range B, the optical spectrum stops broadening and the pulse shape transforms from a square hyperbolic secant shape into a symmetric two-sided inverse exponential shape, with a FWHM relatively constant (pulse FWHM at the beginning and the end of current range B, where shapes are clear, are similar). As we noticed before on Fig. 6, the transition between ranges B and C is obvious in the optical spectrum. Indeed, it strongly narrows (3 times in RMS width) whereas the two symmetric two-sided inverse exponential pulse keeps a constant FWHM, which means that the pulse is far less chirped ($\Delta\nu\Delta\tau$=0.4 at I=180 mA). From the appearance of the Gaussian pedestal on the autocorrelation (I=190 mA), the spectrum FWHM rises, which is also the case in range C1.

2.6. Discussion on optical pulse and spectrum characterization

We have previously distinguished on the RF spectrum two low jitter operation regimes which have been associated with two different optical supermodes SM1 and SM2. However, according to the measurements on the optical spectrum and pulse shape, these two supermodes exhibit

#102295 - $15.00 USD Received 2 Oct 2008; revised 4 Dec 2008; accepted 7 Dec 2008; published 2 Apr 2009

very different pulse shape and optical spectrum properties. SM1, in current range A, corresponds to the classical operation regime of a passively mode-locked laser, i.e. square hyperbolic secant pulse shape with pulse width increasing with current. On the contrary, SM2, in current range C, exhibits a less classical shape, a symmetric two-sided inverse exponential shape. This means that additional non-linear effects are present. What is surprising is that there is no discontinuity in the pulse shape evolution with current whereas there is a clear one in the optical and RF spectra between current range B and C. Concerning the Gaussian pedestal, exponential tails are mandatory in passive mode-locking, and consequently the Gaussian shape of the autocorrelation can only come from a statistical averaging. We attribute this pedestal to unstable satellite pulses corresponding to the supermode SM2, which is consistent with the RF spectrum in range D. It is interesting to note that a fast enlargement of the RF linewidth above a specific power was also theoretically predicted in [29] by using two Hermite-Gauss supermode excitation.

3. Conclusion

We have experimentally analyzed the different regimes of passive mode-locking in a two-section quantum dot laser. In the first range of currents the laser produces low jitter classical square hyperbolic secant pulses associate to supermode SM1 whereas in a second current range it produces low jitter symmetric two-sided inverse exponential pulses associate to supermode SM2. In the intermediate range timing jitter and chirp increase strongly, which is attributed to coupling between main supermode SM1 and weak supermode SM2. The range C, where supermode SM2 is dominant, may be particularly interesting for applications. Indeed, in this range, the laser exhibits 3.5-ps pulses with relatively narrow jitter (narrow RF spectrum) and several mW of average optical power. Moreover Q-switching, whose existence is usually considered as one of the main limits to achieve very short pulses at ultrahigh frequency [31], is observed only near the threshold. For optimization of this laser, it would be important to understand how to obtain good ”single supermode” operation by increasing the repetition rate difference between SM1 and SM2. Finally, a complete characterization of the pulse shape (by spectral phase measurement) is mandatory to confirm the FWHM of the pulse in range C.

Acknowledgments

This research was enabled by the Higher Education Authority Program for Research in Third Level Institutions (2007-2011) via the INSPIRE programme and the authors also gratefully acknowledge the support of Science Foundation Ireland under Contract No. 07/IN.1/I929.

#102295 - $15.00 USD Received 2 Oct 2008; revised 4 Dec 2008; accepted 7 Dec 2008; published 2 Apr 2009